Chain Conformation and Metal···Metal Contacts in Dimers and Stacks of d^8-ML_4 Complexes: Electronic Effects**

Gabriel Aullón and Santiago Alvarez*

Abstract: A qualitative theoretical study is presented of the ligand effects on the strength of the M···M nonbonded interaction in dimers and stacks of d^8-ML_4 chains. It is found that π-acidic ligands enhance and π-basic ligands weaken the M···M bonding interaction. A large amount of structural data can be rationalized with the help of a simple orbital model. Other features of the crystal structures of such compounds are correctly accounted for by semiempirical molecular orbital and electronic band calculations (extended Hückel level). Electronic effects control the deviation from linearity of stacks of complexes with mixed ligands, whereas coupled electronic and steric effects determine the conformational preference. The predictive capability of theoretical band calculations is found to be good.

Keywords
band theory · electronic structure · stacking interactions · square-planar complexes · one-dimensional complexes

Introduction

The enormous interest devoted to stacked square-planar d^8-ML_4 complexes and to their partially oxidized derivatives during the last decades is undoubtedly associated with the possibility of developing one-dimensional systems showing electrical conductivity.[1–6] In fact, the electrical conductivity along the chain direction in these compounds is several orders of magnitude larger than in the perpendicular directions.[1,7,8]

The formation of electronic bands associated with the d_{z^2} metal orbitals was studied by Whangbo and Hoffmann[9] for the case of the tetracyanoplatinate(II) salts, focusing mainly on the bonding and metallic conductivity of the partially oxidized derivatives. Similar studies were reported for the chains of dithiolene and dioximato square-planar d^8 complexes.[10,11] However, the factors that control other structural aspects of these systems, and the influence they might have on optical or electrical properties, have not been systematically studied from a theoretical point of view. Among these factors are the nature of the ligands, the relative rotation of two successive monomers in a chain (measured by the torsion angle τ shown in Scheme 1), and the degree of linearity of the chain (defined by the M-M-M angle θ in Scheme 1).

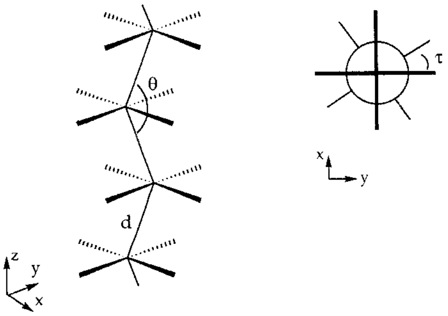

Scheme 1. Parameters defining the geometry of a chain of square-planar d^8-ML_4 complexes.

In this paper we report a theoretical study of the structural aspects mentioned above based on molecular orbital calculations for dimers and band structure calculations for infinite chains, carried out at the extended Hückel level. The only theoretical background that is needed to express the results of our work is a simple qualitative orbital model.[12,13] This model summarizes the metal–metal interaction in the dimers of d^8-ML_4 complexes as the combination of a four-electron repulsion between the d_{z^2} orbitals of the two metal atoms (labeled ① in Scheme 2) and the two attractive donor–acceptor interactions

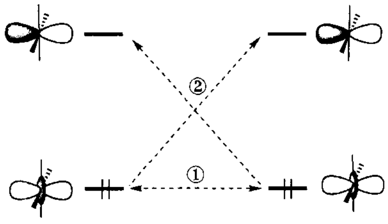

Scheme 2. Model for metal–metal interactions in a dimer of d^8-ML_4 complexes.

---

[*] S. Alvarez, G. Aullón
Departament de Química Inorgànica, Universitat de Barcelona
Diagonal 647, 08028 Barcelona (Spain)
Fax: Int. code +(3)490-7725
e-mail: salvarez@kripto.qui.ub.es

[**] The abbreviations used in this paper are given in the Appendix.

between the d_{z^2} orbital of one metal atom and the p_z orbital of the other one (labeled ② in Scheme 2). For a given dimer, the relative weights of the two interactions determines whether a net bonding situation results or not.

Results and Discussion

π-Acidic Character of the Ligands: We look first at the possible influence of the π-basic or π-acidic character of the ligands on the strength of the metal–metal interactions from a theoretical point of view. The results will then be compared with experimental data. Extended Hückel molecular orbital calculations were performed for dimeric complexes with different proportions of π-basic and π-acidic ligands: $[Rh_2Cl_8]^{6-}$, $[Rh_2Cl_4(CO)_4]^{2-}$ (*cis* and *trans*), and $[Rh_2(CO)_8]^{2+}$ in the two extreme conformations (Scheme 3), eclipsed ($\tau = 0°$) and staggered ($\tau = 45°$). We evaluate the strength of the metal–metal interaction through the calculated Rh$\cdots$Rh overlap populations presented in Figure 1. A clear picture emerges: the Rh$\cdots$Rh contact strengthens as the number of π-acidic ligands increases. The analysis of the different contributions to the overlap population indicate that the π-type interactions are destabilizing, the δ-type interactions are practically negligible, and the σ interactions are responsible for the positive Rh$\cdots$Rh overlap population and for its dependence on the number of π-acidic ligands. We will therefore start by analyzing the bonding σ interactions. Later on we will discuss the effect of the destabilizing π interactions on the relative arrangement of successive monomers.

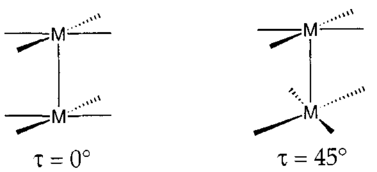

Scheme 3. Eclipsed and staggered conformations of the dimer.

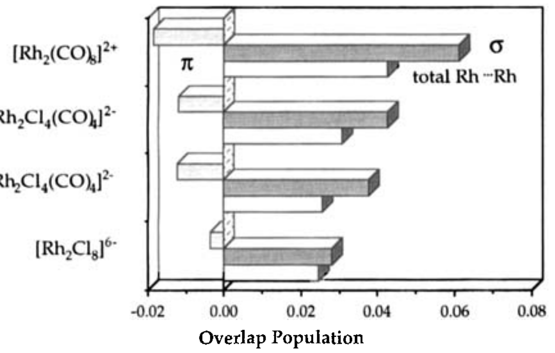

Figure 1. Calculated Rh$\cdots$Rh overlap population for several dimeric Rh^I complexes (white bars) in a staggered conformation. The σ contributions are represented by the darkly shaded bars and the π contributions by the lightly shaded bars.

We now analyze the changes in our simplified orbital model (Scheme 2) induced by the introduction of π-acidic ligands, in order to understand the mechanism by which they strengthen the σ metal–metal interaction. In Figure 2 (left), the HOMO and LUMO of the monomer $[RhCl_4]^{3-}$ are shown. These σ-type orbitals are a_{1g} (93% d_{z^2} of Rh) and $2a_{2u}$ (100% p_z of the metal, situated 8 eV above the HOMO in our calculations), respectively. The LUMO is destabilized with respect to that for σ-donor ligands, because of the interaction with the π-type lone-pair orbital of the chlorides. In $[Rh(CO)_4]^+$ (Figure 2, right), the composition of a_{1g} is unchanged, but the π^*_{CO} orbitals of the ligands mix with and stabilize p_z. The outcome is the presence of some metal p_z contribution to the π^*_{CO} orbital ($1a_{2u}$), which now lies much closer in energy to the HOMO (2 eV in our calculations) than in $[RhCl_4]^{3-}$.[14] Even if this orbital is centered on the carbonyl ligands, it has a sizeable contribution from the Rh atom (16% in our calculations).[15–17] Obviously, the presence of the $1a_{2u}$ orbital in the $[Rh(CO)_4]^+$ monomer affects the orbital interaction in the dimer. Thus, in presence of π-acidic ligands the interaction model (Scheme 2) must be modified as shown in Scheme 4.

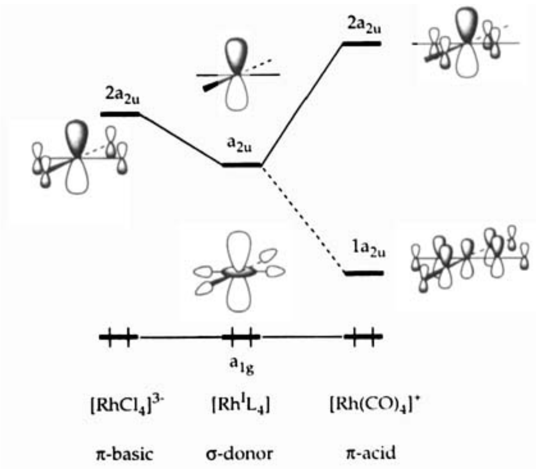

Figure 2. Schematic diagram of the effect of the ligand's π orbitals on the frontier orbitals of a Rh^IL_4 complex with only σ-donor ligands (middle): π-basic ligands, $[RhCl_4]^{3-}$ (left), and π-acidic ligands, $[Rh(CO)_4]^+$ (right).

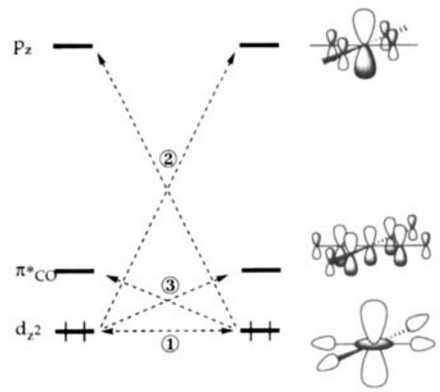

Scheme 4. Interaction model for complexes with π-acidic ligands (modified from Scheme 2).

In order to discuss in some detail the new orbital interaction model (Scheme 4), we analyzed the $\sigma(M\cdots M)$ overlap population in terms of the three contributions shown in Scheme 4 (Figure 3) for several homoleptic complexes of Rh^I and Pt^{II}. Since the a_{1g} orbital is not affected by substitution of the carbonyl ligands by chlorides, the repulsion ① between the d_{z^2} electrons is similar for different sets of ligands. Only a slight decrease in the repulsive interaction is found for the better σ-donor ligands (e.g., CN^- and CO), due to a stronger $s+d_{z^2}$ hybridization. On the other hand, part of the attractive $M\cdots M$ interaction ② becomes a metal-mediated donor–acceptor interaction ③ between the d_{z^2} orbital of one monomer and the appropriate symmetry-adapted combination of the π^*_{CO} orbitals. Despite the small contribution of $p_z(M)$ to the $2a_{2u}$ MO, this new type of interaction induced by π-acidic ligands is more stabilizing than ② because of the much smaller energy difference between the interacting orbitals. By comparing the data for the cyano or carbonyl complexes with those for the chloro analogues of the same metal, we see that the strengthening of the metal–metal bonding interaction upon incorporation of π-acidic ligands is essentially due to the presence of the new donor–acceptor interactions ③.

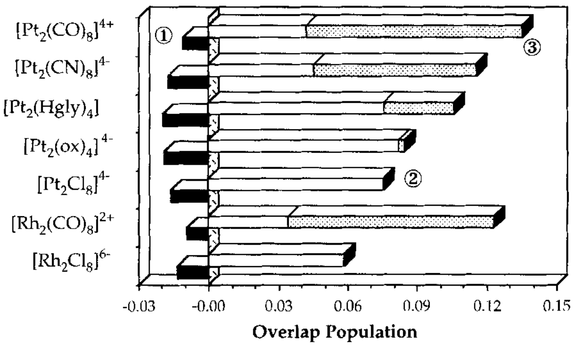

Figure 3. Analysis of the σ part of the $Rh\cdots Rh$ overlap population in eclipsed homoleptic Rh^I and Pt^{II} dimers in terms of the three orbital contributions shown in Scheme 4: four-electron repulsion (①, black bars), direct donor–acceptor interaction between d_{z^2} of one metal and p_z of the other one (②, white bars), and metal-mediated donor–acceptor interaction between metal d_{z^2} orbital of one monomer and the A_{2u} combination of the π^*_{CO} orbitals of the other monomer (③, shaded bar).

Can these trends actually be found in the experimental structural data? Although the structures of some of the molecules used for our calculations are not known, the model described above relies only on the topology of the molecular orbitals of square-planar complexes and on the very nature of the π-acidic ligands. Hence our qualitative conclusions can be applied to square-planar complexes of any transition metal ion with a variety of ligands. Let us take a look at some structural data, even though a more detailed discussion will be presented in the next section. In $K_2[PtCl_4]$, the Pt atoms in the stacks of $[PtCl_4]^{2-}$ anions are separated by 4.11 Å,[18] whereas in the salts of $[Pt(CN)_4]^{2-}$ the $Pt\cdots Pt$ distances are much shorter, between 3.1 and 3.7 Å[19] (between 3.6 and 3.7 Å for chains with the same conformation[20–22], Table 1). In fact, the long $Pt\cdots Pt$ distance in the salt of the tetrachloroplatinato(II) ion suggests that this is not a bonding interaction, in agreement with the fact that the electronic spectra in solution and in the solid state are more or less identical.[23, 24] A related observation is that the $[Ru(CO)_4]$ complex shows a comparatively short $Ru\cdots Ru$ distance of 2.86 Å.[25]

Table 1. Structural parameters of stacks of d^8-ML_4 complexes with monodentate ligands (see Scheme 1 for the definition of τ and θ).

Compound	$M\cdots M$ (Å)	τ (°)	θ (°)	Ref.
$[Ru(CO)_4]$	2.860	41	180	[25]
$[RhCl(CO)_2(Me\text{-}im)]$	3.283	54	169	[26]
$[RhCl(CO)_2(Hpz)]$	3.452	180	177	[27]
$[IrCl(CO)_3]$	2.844	45	179	[28]
$[IrBr(CO)_3]$	2.854	45	178	[29]
$[Ni(CN)_4]^{2-}$	3.364	45	180	[30]
$[Ni(CN)_4]^{2-}$	3.387	27	180	[31]
$[Pd(CN)_4]^{2-}$	3.730	17	180	[32]
$[Pd(CN)_4]^{2-}$	3.689–3.795	0	161, 165	[33]
$[Pt(CN)_4]^{2-}$	3.155	45	180	[34]
$[Pt(CN)_4]^{2-}$	3.263	34	176	[35]
$[Pt(CN)_4]^{2-}$	3.321	45	180	[34,36]
$[Pt(CN)_4]^{2-}$	3.380	30	180	[34]
$[Pt(CN)_4]^{2-}$	3.421	32	176	[37,38]
$[Pt(CN)_4]^{2-}$	3.478	16	180	[39]
$[Pt(CN)_4]^{2-}$	3.545	33	156	[40,41]
$[Pt(CN)_4]^{2-}$	3.603	0	180	[34]
$[Pt(CN)_4]^{2-}$	3.690	17	180	[42]
$[Pt(CN)_4]^{2-}$	3.651–3.754	0	162, 166	[21,22]

Since a large amount of available structural data corresponds to complexes of bidentate ligands, we now analyze the effect of some of those ligands using the orbital model in Scheme 4, before continuing our discussion of the structural data. Among the most common chelating ligands in chains of d^8-ML_4 complexes are the β-diketonates,[43–50] oxalates,[51–57] *vic*-dioximates,[58] and dithiocarboxylates.[59] Let us now look at the molecular orbitals of the homoleptic complexes [M(chelate)$_2$] and how they might affect the $M\cdots M$ interactions (Table 2). Later on we will study the mixed-ligand complexes of type $[MX_2(\text{chelate})]$ (Table 3).

The analysis of the $\sigma(M\cdots M)$ overlap population for the dimer $[Pt_2(ox)_4]^{4-}$ (Figure 3) and of the composition of its molecular orbitals shows that the oxalato ligand has very little

Table 2. Structural data for homoleptic polynuclear and chain complexes of the platinum group with oxalato or glyoximato ligands.

Compound	$M\cdots M$ (Å)	τ (°)	θ (°)	Ref.
$[Ni(Hbzgly)_2]$	3.180	68	180	[60]
$[Ni(Hdmg)_2]$	3.245	90	180	[61]
$[Ni(Hbzgly)_2]$	3.856	0	180	[62]
$[Ni(Me\{NH_2\}Hgly)_2]$	3.915	0	180	[63]
$[Ni(\{NH_2\}_2Hgly)_2]$	3.969	0	180	[64]
$[Pd(Hgly)_2]$	3.244	90	180	[65]
$[Pd(Hdmg)_2]$	3.250	90	180	[58]
$[Pd(\{C_4H_3O\}_2Hgly)_2]$	3.465	87	180	[66]
$[Pd(\{NH_2\}_4H_3gly_2)]^+$	3.543	5	180	[67]
$[Pd(Hgly)_2]$	3.558	0	180	[68]
$[Pd(\{NH_2\}_2Hgly)_2]$	3.899	0	180	[69]
$[Pt(Hbzgly)_2]$	3.173	87	180	[70]
$[Pt(Cl_2Hgly)_2]$	3.176	67	180	[71]
$[Pt(Hdmg)_2]$	3.256	90	180	[58, 72]
$[Pt(Hbzgly)_2]$	3.386	22	180	[73]
$[Pt(Hgly)_2]$	3.504	0	180	[74]
$[Pt_3(\{NH_2\}_{12}H_4gly_6)]^{4+}$	3.639	3	180	[75]
$[Pt(\{NH_2\}_2H_2gly)_2]^{2+}$	3.660	0	180	[76]
$[Pd(ox)_2]^{2-}$	3.700	0	180	[77]
$[Pt(ox)_2]^{2-}$	3.660	0	180	[53]
$[Pt(\{NH_2\}_2H_2gly)_2][Pt(ox)_2]$	3.623, 3.826	8	134	[76]
$[Ni(\{NH_2\}_2H_2gly)_2][Pt(ox)_2]$	3.673	0	180	[78]

Table 3. Structural data for mixed-ligand polynuclear and chain compounds of Rh^{I}, Ir^{I}, Pd^{II} and Pt^{II} with one chelating ligand. Ligands marked with an asterisk are derivatives of acetylacetonato.

Compound	M···M (Å)	τ (°)	θ (°)	Ref.
$[Rh(ox)(CO)_2]^-$	3.243	180	175	[51]
$[Rh(acac)(CO)_2]$	3.253, 3.271	180	175	[43, 46, 79]
$[Rh(MePhDtc)(CO)_2]$	3.253	132	180	[80]
$[Rh(\{MeCNH\}_2CH)(CO)_2]^+$	3.271, 3.418	180	164	[44]
$[Rh_2(gcamph^*)(CO)_4]$	3.313, 3.373	78, 121	164	[50]
	3.419, 3.643	81, 119	159	
$[Rh(menth^*)(CO)_2]$	3.332, 3.401	180, 142	164	[49]
$[Rh_3(ttz)Cl_2(CO)_6]$	3.397, 3.229, 3.459	12, 44, 4	176, 168	[81]
$[Rh_3(tz)Cl_2(CO)_4(tfbb)]$	3.425	110	177	[82, 83]
$[Rh_2(pz)Cl(CO)_4]$	3.511, 3.620	26, 27	169	[84]
$[Ir(acac)(CO)_2]$	3.200	180	180	[43]
$[Ir_2(mdcbi)(CO)_4]^-$	3.361, 3.299	86, 180	168	[85]
$[RhIr(acamph^*)(CO)_4]$	3.362, 3.440	135, 173	170	[48]
$[Pd(bipy)Cl_2]$	3.460	180	162	[86]
$[Pd(bph)(CO)_2]$	3.243	180	162	[87]
$[Pd(bipy)(CN)_2]$	3.354	180	180	[88]
$[Pt(bipy)Cl_2]$	3.448	180	161	[89]
$[Pt(bipy)(CN)_2]$	3.346	180	169	[88, 90]

π-acidic character, hence very little strengthening effect on the M···M contact. The practically negligible contribution of interaction ③ in the case of the oxalato ligand can be ultimately explained by the higher electronegativity of its oxygen donor atoms. Effectively, this ligand has empty π* molecular orbitals, but their mixing with the metal p_z orbital is minute, since they are mostly localized at the carbon atoms (Scheme 5). It should be stressed that the small changes in the destabilizing contribution ① are associated with the extent of the delocalization of the d_{z^2} orbital: for less electronegative donor atoms, this orbital is more delocalized and the d_{z^2}/d_{z^2} repulsion diminishes. On the other hand, the glyoximato ligand in $[Pt_2(Hgly)_4]$ shows stronger mixing of $p_z(M)$ with a ligand π* orbital (Scheme 5) and the interaction of type ③ is important, resulting in a strengthening of the M···M interaction (Figure 3). An analysis of the available structural data in the light of the present results will be carried out in the next section.

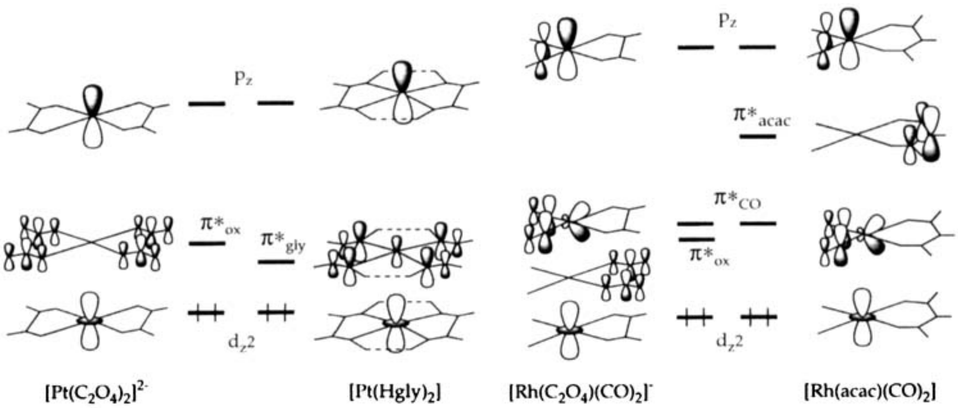

Scheme 5. Molecular orbitals corresponding to Scheme 4 for the homoleptic complexes $[M(chelate)_2]$ and mixed-ligand complexes of type $[M(chelate)X_2]$.

In contrast to the bidentate ligands in the other complexes studied above, the dithiocarboxylato ligands bridge two metal atoms rather than forming chelates. A previous ab initio MO study[91] showed that, even if the Pt···Pt interaction is weak,

Table 4. Structural data for chain complexes of d^8 transition metals with dithiocarboxilato ligands. The interdimer parameters are given in parentheses.

Compound	M···M (Å)	τ (°)	θ (°)	Ref.
$[Ni_2(PhCH_2CS_2)_4]$	2.551 (3.497)	28 (42)	180	[92, 93]
$[Pd_2(PhCH_2CS_2)_4]$	2.715 (3.297)	26 (44)	180	[92, 93]
$[Pd_2(MeCS_2)_4]$	2.739 (3.257)	24 (48)	180	[94]
$[Pd_3(MeCS_2)_6]$	2.754 (3.399)	21 (34)	180	[94]
$[Pt_2(PhCH_2CS_2)_4]$	2.765 (3.238)	25 (46)	180	[59]
$[Pt_2(MeCS_2)_4]$	2.767 (3.776, 3.819)	1 (1, 2)	152	[95]
$[Pt_2(Me_2CHCS_2)_4]$	2.795 (3.081)	30 (41)	180	[96]
$[Pt_2(HexCS_2)_4]$	2.855 (3.224)	27 (27)	180	[97]

the presence of a π*(SCS) orbital,[17] capable of interaction with $p_z(M)$, results in a small Pt···Pt overlap population. Of course, the short intramolecular Pt···Pt distances cannot be solely ascribed to electronic effects; the geometrical constraint imposed by the bridging ligands is also important. However, the intermolecular distances (Table 4) are similar to those in the unsupported complexes studied above, in agreement with the existence of some bonding interaction.

For the study of the orbital model in Scheme 4 applied to mixed-ligand complexes of type $[M(chelate)X_2]$, several dimers of Rh^{I} were considered (Figure 4). It is apparent that the σ-stabilizing contributions ② and ③ increase with the number of π-acidic ligands, as expected from the discussion of the results for the homoleptic complexes. A notable difference, however, is that, in the mixed-ligand complexes $[M(chelate)(CO)_2]$, the lower symmetry allows mixing of not only $p_z(M)$ but also $d_{xz}(M)$ into the π^*_{CO} empty orbitals, resulting in a hybridization at the metal atom as shown in Scheme 5. We will show below that this symmetry-imposed orbital mixing is of great importance in determining the departure from linearity of the chain.

As found before for the bis(oxalato)platinate complex, mixing of the π* molecular orbitals of the chelating ligand with p_z of the metal is very small in $[M(chelate)X_2]$ (chelate =

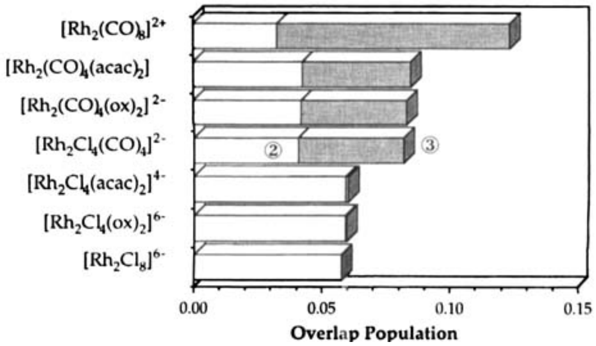

Figure 4. Stabilizing contributions to the σ(Rh···Rh) overlap population (see Scheme 4) for dimers of mixed-ligand Rh^{I} complexes. Data for the homoleptic complexes $[Rh_2(CO)_8]^{2+}$ and $[Rh_2Cl_8]^{6-}$ are also shown for comparison. Calculations were performed with a rotated (τ = 180°) conformation with Rh···Rh = 2.9 Å.

oxalato or acetylacetonato) (Scheme 5), in agreement with NMR experimental data.[44] The corollary of our results is that the π-acidic ligands have a stabilizing effect on the $\sigma(M\cdots M)$ interaction, which decreases in the order $CO > CN^- > Hgly^- > ox^{2-} > acac^- \approx Cl^-$, according to the decreasing participation of the $p_z(M)$ atomic orbital in the $\pi^*(L)$ MO (see, e.g., Scheme 4). It should be mentioned that this contribution has been experimentally detected in the charge-transfer transition $d_{z^2} \rightarrow \pi^*(Hgly^-)$.[98]

So far we have discussed only the bonding part of the $M\cdots M$ interaction, that is, the σ contributions. The repulsive π interactions between the occupied orbitals, however, are also sensitive to the nature of the ligands and can also affect the overall strength of the $M\cdots M$ contact. In Figure 1 it can be seen that the π $M\cdots M$ repulsion is stronger for carbonyl than for chloride. This difference can be traced back to the interaction between the d_{xz} (or d_{yz}) orbital of one monomer and the σ-bonding MO's involving the p_x (or p_y) metal orbital of the other monomer (Scheme 6). There are two reasons for the stronger repulsion in the case of the carbonyl complex. Firstly, there is the larger contribution of the metal p orbital in the σ-bonding MO, due to the better σ-donor ability of the ligand. Secondly, the p_z orbitals of the carbonyl ligands contribute to the overlap between the two fragment orbitals shown in Scheme 6, owing to their π-acidic nature, whereas the the d_{xz}/p_x overlap is in part compensated for by the negative overlap between the ligands' orbitals in the case of chloride. In the case of mixed-ligand complexes, the π-type orbitals are important for the determination of the chain conformation, but we defer a more detailed discussion to the corresponding sections below.

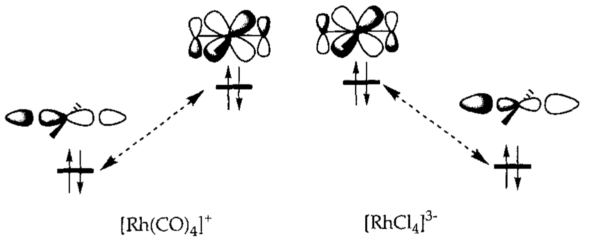

Scheme 6. Explanation of the difference in π $M\cdots M$ repulsion in $[Rh_2Cl_8]^{6-}$ and $[Rh_2(CO)_8]^{2+}$.

Structural Trends: We now examine the structural data from the literature, and compare it with the expected influence of the π-acidity of the ligands discussed in the previous section. In the structural data presented in Tables 1–3, it is interesting to note that the shortest $M\cdots M$ distances correspond to the neutral complexes having carbonyl ligands with a staggered conformation ($\tau \approx 45°$), such as $[IrX(CO)_3]$ and $[Ru(CO)_4]$. The presence of other ligands, such as pyrazole or imidazole, results in longer $M\cdots M$ distances, possibly due to a combination of electronic (poorer π-acidic character) and steric reasons. Octakis(isonitrile) complexes of Rh^I also present distances in the range 3.19–3.29 Å;[99–101] only when the ligand is the bridging 1,8-diisocyanomenthane does the long spacer between the two nitrile groups prevent the short contact favored by the π-acidic ligand ($M\cdots M$ 4.48 Å).[102]

The shortest $Pt\cdots Pt$ distances in the Pt chains (3.15–3.26 Å, Tables 1 and 2) are found in some of the salts of $[Pt(CN)_4]^{2-}$ and in some of the $[Pt(dioximato)_2]$ complexes, in excellent agreement with the order of π-acceptor strengths discussed above (see Figure 3). The fact that some complexes with the same or similar ligands contain longer distances might be related to the different internal angles, discussed below. The oxalato complexes have markedly longer $M\cdots M$ distances as expected from the weak π-acidic character of this ligand. The rather short $M\cdots M$ distances (2.84–3.01 Å) found in several bis(oxalato)platinates must be attributed to the partial oxidation of the Pt atom in such complexes,[54–57] which changes the destabilizing nature of interaction ① into a bonding one.

The data for the mixed-ligand complexes (Table 3) confirm our theoretical prediction that the $M\cdots M$ distance should decrease with the number of π-acidic ligands. Hence, the $Ir\cdots Ir$ distance of 3.20 Å in $[Ir(acac)(CO)_2]$ contracts to 2.85 Å in a compound with one more carbonyl ligand, $[IrX(CO)_3]$. In contrast, the $M\cdots M$ distances in the $[Rh(chelate)(CO)_2]$ complexes (3.24–3.64 Å) are similar to those in the analogous complexes $[RhX(CO)_2L]$ (3.28 and 3.45 Å, Table 1). Note also that the $M\cdots M$ distances are clearly shorter in $[M(bipy)(CN)_2]$ than in the corresponding $[M(bipy)Cl_2]$ analogues (M = Pd, Pt). Still shorter is the $Pt\cdots Pt$ distance in the recently reported carbonyl complex $[M(bph)(CO)_2]$,[87] indicating a stronger π-acidic character of CO compared to the cyanide group.

Surprisingly, the $M\cdots M$ distance is practically identical for complexes with the same ligands and different metals. This distance is probably influenced by the ligand–ligand repulsions,[3] as well as by the interaction with counterions or with molecules of hydration:[2, 3, 6, 19] 3.36–3.42 Å in $Ca[M(CN)_4]\cdot 5H_2O$ (M = Ni, Pd, Pt); 3.25–3.26 Å in $[M(Hdmg)_2]$ (M = Ni, Pd, Pt); 3.26 and 3.20 Å for Rh and Ir in $[M(acac)(CO)_2]$.

Rotational Conformation: One may be tempted to invoke steric effects to explain the conformation of the chains, defined by the angle τ (Scheme 1). Indeed, the data in Tables 1–4 indicate that the eclipsed conformation ($\tau = 0°$) is rarely observed, as would be expected based on steric repulsion. However, the calculations indicate that, even when the steric bulk of the substituents (e.g., in $acac^-$ or $Hgly^-$) is minimized, some conformations are more stable than others, and these conformations are strongly dependent on the nature of the ligands present. In this section we discuss the results of the optimization of the torsion angle for the dimeric and chain models of several chain compounds.

We started by looking at the homoleptic complexes $[M_2Cl_8]^{n-}$, $[M_2(CO)_8]^{n+}$, and $[Pt(CN)_4]^{2-}$, where M = Rh^I or Pt^{II}, for which we optimized the torsion angle τ at a fixed $M\cdots M$ distance in a dimer (EH calculations) and in a regular chain with two monomers per repeat unit (EHTB calculations). Our results (Table 5) indicate that the staggered conformation is most stable in these examples and also shows the strongest $M\cdots M$ interaction, as previously reported by Hoffmann et al.[103] This preference is much more pronounced for the chloro complexes, for which high rotation barriers are calculated.

Although we will see later that electronic effects also have an influence on the conformational choice, let us first look at the *steric* factors in the homoleptic complexes by looking at the intermolecular ligand–ligand interactions. Figure 5 shows the

Table 5. Optimized values for the internal torsion angle τ and rotational barriers (in parentheses, kcal mol^{-1}) for several dimers and chains of Rh^I and Pt^{II}. For mixed-ligand complexes, for which two minima are found, the relative energy of the second minimum is given in square brackets (kcal mol^{-1}).

Compound	Dimer (2.9 Å)	Chain (2.9 Å)	Chain (3.3 Å)
$[RhCl_4]^{3-}$	45 (56.1)	45 (108.9)	45 (20.0)
$[Rh(CO)_4]^+$	45 (1.7)	45 (3.7)	45 (0.3)
trans-$[RhCl_2(CO)_2]^-$	52 (31.4)	48 (53.4)	51 (10.7)
cis-$[RhCl_2(CO)_2]^-$	140 (31.8)	138 (56.7)	140 (11.6)
	48 [2.0]	47 [0.9]	48 [0.8]
$[Rh(acac)Cl_2]^{2-}$	51 (36.2)	50 (61.5)	50 (13.9)
	180 [5.6]	180 [17.2]	180 [1.3]
$[Rh(ox)Cl_2]^{3-}$	50 (30.6)	47 (46.5)	52 (10.5)
	146 [0.8]	163 [7.8]	150 [−0.5]
$[Rh(acac)(CO)_2]$	79 (8.8)	59 (12.0)	86 (4.6)
	180 [0.2]	180 [2.2]	180 [−0.5]
$[Rh(ox)(CO)_2]^-$	63 (2.1)	0 (8.1)	0 (0.2)
	180 [0.3]	180 [6.3]	180 [−0.7]
$[PtCl_4]^{2-}$	45 (56.1)	45 (112.2)	45 (20.6)
$[Pt(CN)_4]^{2-}$	45 (9.2)	45 (17.8)	45 (3.0)
$[Pt(CO)_4]^{2+}$	45 (1.8)	45 (2.8)	45 (0.4)
$[Pt(Hgly)_2]$	90 (6.2)	90 (5.3)	90 (2.5)
$[Pt(ox)_2]^{2-}$	90 (2.8)	90 (5.5)	90 (0.7)
$[Pt_2(\mu\text{-}HCS_2)_4]$ [a]	22 (13.8)	28 (80.1)	26 (55.0)
$[Pt_2(\mu\text{-}HCS_2)_4]$ [b]		45 (92.7)	45 (20.8)

[a] Intramolecular. [b] Intermolecular.

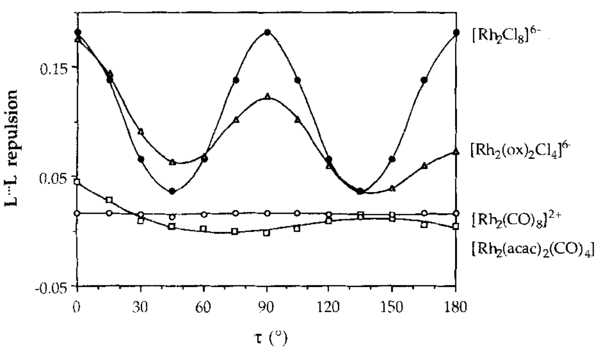

Figure 5. Ligand···ligand repulsion (negative overlap population) as a function of the internal torsion angle τ calculated for several Rh^I dimers (Rh···Rh = 2.9 Å): $[Rh_2Cl_8]^{6-}$ (●), $[Rh_2(CO)_8]^{2+}$ (○), $[Rh_2(ox)_2Cl_4]^{6-}$ (▲) and $[Rh_2(acac)_2(CO)_4]$ (□).

repulsion (as the negative overlap population) for several ligand sets (i.e., without the metal atoms) in the model dimers as a function of the internal torsion angle. The main conclusion from this plot is that the ligands with light donor atoms (C, O, N) give smaller repulsions, and hence small barriers to rotation and less marked conformational preference, whereas the heavier donor atoms (Cl, S) give rise to strong repulsions when eclipsed. In summary, the preferred conformations are those in which the light atoms of the ligands in two successive monomers are not eclipsed and the heavy atoms are as far apart as possible from each other. In fact, it has been recognized for some time that small, planar ligands are a prerequisite for the existence of chains of d^8-ML_4 complexes.[3, 6, 39] All other things being equal, the conformational preference is, as expected, much weaker at longer M···M distances.

If we now compare these results with the experimental data, we find that, in the salts of the $[MCl_4]^{2-}$ (M = Pt, Pd)[18, 104, 105] anions, the successive monomers are in an eclipsed conformation. This apparent contradiction can be explained by the long M···M experimental separations. Possibly the existence of the alkaline cations *bridging* the chloride ions of consecutive monomers also favor the eclipsed conformation. For the carbonyl and cyano complexes, for which a staggered conformation is also expected (τ = 45°), the experimental data is in excellent agreement with the theoretical prediction. Hence, $[IrCl(CO)_3]$ and $[IrBr(CO)_3]$ are staggered and $[Ru(CO)_4]$ is nearly staggered. Similarly, a nearly staggered conformation is predicted to be the most stable one for the mixed-ligand complexes $[RhCl_2(CO)_2]^-$, and is experimentally found for $[RhCl(CO)_2(Me\text{-}im)]$ (Table 1).

In the salts of the anionic $[M(CN)_4]^{2-}$ complexes (M = Ni, Pd, Pt), a nearly staggered conformation is most common, similarly to what is predicted for the analogous carbonyl complexes. However, in many cases the structure is far from being staggered, and an eclipsed conformation has even been reported for three salts (Table 1). The variation in the internal torsion angles has been attributed to the presence of different cations and water of hydration.[6] However, it should be noted that the compounds with shorter M···M distances adopt a staggered structure, while only those with long M···M distances (i.e., larger than 3.4 Å) are eclipsed. This is in agreement with our calculations (Table 5), which predict a quite flat potential for rotation at a Pt···Pt separation of 3.3 Å in the chain of $[Pt(CN)_4]^{2-}$. In $[Rh_2(pz)Cl(CO)_4]$ and $[Rh_3(ttz)Cl_2(CO)_6]$ long metal–metal distances also coexist with torsion angles that are smaller than expected (Table 3).

For the bis(dioximato) and bis(oxalato) Pt complexes, all possible conformations are found in the range $0 \leq \tau \leq 90°$. The calculations for a model dimer and for a one-dimensional stack both predict a conformation with τ = 90° to be most stable. However, there are many examples in Table 2 of complexes with the eclipsed conformation (τ = 0°). A closer look at the structural data shows that the compounds with shorter M···M distances (i.e., M···M < 3.5 Å) adopt the expected conformation. If, as stated above, intermolecular ligand–ligand repulsions have an influence on the chain conformation, it is not surprising that the conformational preference is less pronounced at longer distances, with other factors eventually favoring the eclipsed conformation. These ideas are supported by band calculations on the $[Pt(ox)_2]^{2-}$ chain at the two limiting conformations (τ = 0 and 90°). As seen in the one-electron energy curves presented in Figure 6, the optimized Pt···Pt distance for the rotated conformation is 3.4 Å, whereas for the eclipsed conformation a longer distance (3.6 Å) is

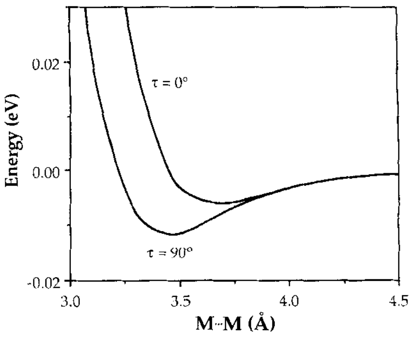

Figure 6. Calculated (EHTB) one-electron relative energy as a function of the M···M distance for a chain of $[Pt(ox)_2]^{2-}$ in the eclipsed (τ = 0°) and rotated (τ = 90°) conformations.

preferred. It can also be seen that the energy difference between the two conformations is minute at long distances, but larger at short distances.

For the case of the bridged tetrakis(dithiocarboxilato) dimeric complexes of Pt, the conformational angles are constrained by the bridging ligands. If we model such compounds based on the metal atoms and their first coordination spheres, as in $[Pt_2S_8]^{12-}$, the calculations yield the staggered confomation ($\tau = 45°$) as the most stable one, as found for $[Pt_2Cl_8]^{4-}$. In agreement with this result, the interdimer torsion angles are close to 45° in most cases (Table 4). The tendency to avoid the eclipsed conformation is dramatically reflected in the intradimer torsion angles. In fact, optimization of the conformation in a dimeric $[Pt_2(HCS_2)_4]$ complex yields $\tau = 22°$, in excellent agreement with the experimental values ($\tau = 19–30$, Table 4). Also the optimized S–S bite (3.03 Å) and the bond angle of the dithiocarboxylato group (SCS = 129°) are in excellent agreement with the experimental values.[97]

The preference for noneclipsed conformations is not purely steric. Electronic and steric factors are coupled. When chloro ligands are present, the M···M overlap population is seen to increase upon departure from the eclipsed geometry, a change which is due to the σ component through interaction of type ② and, to a lesser extent, through interaction ①. This is so because the overlap between the $2a_{2u}$ and a_{1g} orbitals (Figure 2) of neighboring molecules is smaller in the eclipsed conformation, as a result of the interaction between the atomic orbitals of the ligands (see Scheme 7). For interaction ①, a more effective overlap between ligands in the eclipsed conformation results in a stronger repulsion, which disfavors such a geometry. Note that a similar coupling of metal- and ligand-destabilizing interactions is also present in the π interactions (Scheme 6). Hence, the *steric* interligand repulsions can be modulated electronically by the appropriate choice of the nature of the ligands.

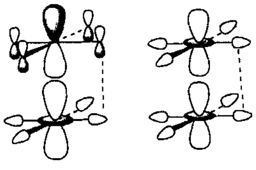
Scheme 7. Interaction between the atomic orbitals of the ligands in the eclipsed conformation of MCl_4 dimers.

For the model complexes $[Rh_2(chelate)_2(CO)_4]$ (where chelate stands for acetylacetonato or oxalato), two low-energy conformations are found, which coincide with two maxima in the M···M overlap population. At large Rh···Rh separation, the geometry with the lowest energy is that with $\tau \approx 180°$ (see Table 5). In keeping with our results, the experimental angle in the chain compounds $[Rh(ox)(CO)_2]^-$ and $[Rh(acac)(CO)_2]$ is 180° (Table 3). Other β-diketonate complexes of Rh^I also have torsion angles close to one of the two theoretical minima. In a few cases, a large deviation from the expected torsion angle is observed, though it is invariably associated with a very long M···M distance (3.6 Å) or with the presence of bridging ligands.[45, 50] It is noteworthy that in $[Ir_2(mdcbi)(CO)_4]^-$ the two independent Ir···Ir contacts give torsion angles in excellent agreement with the minima found for analogous distances in the $[Rh_2(acac)_2(CO)_4]$ chain. In this case the preferred conformation is one in which the ligands of successive units in the chain are superimposed, which cannot be explained in terms of steric effects.

As we have seen above, the acetylacetonato and oxalato ligands have a practically negligible π-acidic character. Hence, the π-acidic character of the CO ligands in $[Rh_2(chelate)_2(CO)_4]$ induces an asymmetry in the π-type molecular orbitals, depicted in Scheme 8. In particular, the d_{xz} atomic orbital is hybridized through mixing with p_z, acquiring more bonding character toward the CO π^* orbitals, with which it combines in a bonding way in an occupied MO. In contrast, in the antibonding combination of the empty MO, d_{xz} is hybridized away from the carbonyls. With this orbital topology, it is now clear that in the carbonyl-over-chelate conformation ($\tau = 180°$) the occupied π orbital of one molecule interacts best with the empty π orbital of a neighboring monomer (Scheme 9, left), thus providing some stabilization to that conformation. On the other hand, in the fully eclipsed conformation ($\tau = 0°$), the occupied π orbitals of successive monomers interact with each other, resulting in four-electron repulsions (Scheme 9, right).

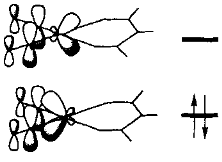
Scheme 8. The π-type molecular orbitals in $[Rh_2(chelate)_2(CO)_4]$, where the chelating ligand is acetylacetonato or oxalato.

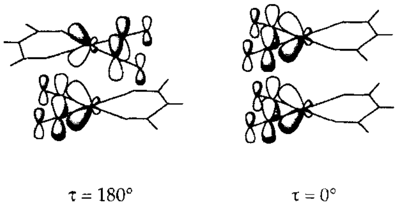

Scheme 9. Interaction between π orbitals (Scheme 8) of successive monomers in the carbonyl-over-chelate and eclipsed conformations.

Nonlinearity of the Chains: The structural data reveals that in some cases the chains deviate significantly from linearity, that is, the bond angle θ (Scheme 1) is smaller than 170° (see Tables 3 and 6). We have analyzed this structural phenomenon, in search for an explanation. Steric, geometric, and electronic effects in

Table 6. Structural parameters for compounds of nuclearity n with bridging ligands and $d^8 \cdots d^8$ contacts.

Compound	n	M···M (Å)	τ (°)	θ (°)	Ref.
$[Rh_2(hp)_2(CO)_4]$	∞	2.899, 3.411	22, 144	151, 175	[106]
$[Au_2(Ph_2P\{CH_2\}_2)_2Cl_4]$	∞	3.091, 3.692	43, 44	154, 160	[107]
$[Rh_3(hnapy)_2(CO)_2(cod)_2]^-$	3	2.907, 2.912	18, 19	168	[108]
	3	2.910, 2.911	19, 18	168	
$[Rh_3(dpmp)(MeCN)_6]^{3+}$	3	3.089, 3.107	0, 0	160	[109]
$[Pd_3(MeCO_2)_4Ph_2(SbPh_3)_2]$	3	3.012	13	180	[110]
$[Pd_2(MeCO_2)_2(bomp)_2]$	4	2.842, 3.183	4, 180	173	[111]
$[Pd_2(MeCO_2)_2(btmp)_2]$	4	2.871, 3.200	2, 180	174	[111]
$[Pd_2(hp)_2(en)_2]$	4	2.982, 3.220	26, 180	160	[112, 113]
$[Pt_2(hp)_2(NH_3)_4]^{2+}$	4	2.877, 3.129	20, 180	158	[114, 115]
$[Pt_2(meu)_2(NH_3)_2(bipy)]^{2+}$	4	2.929, 3.489	13, 180	166	[116]
$[Pt_4(MeCO_2)_6(NO)_2]$	4	2.944, 3.300	14, 180	156	[117]
$[Pt_2(hp)_2(en)_2]^2 +$	4	2.992, 3.236	25, 180	161	[118]
$[Pt_4(pyrr)_4(NH_3)_8]^{4+}$	4	3.033, 3.186	1, 180	158	[119]
$[Pt_2(pyt)_2(en)_2]^{2+}$	4	3.083, 3.613	33, 180	152	[120, 121]
$[Pt_2(mpyt)_2(en)_2]^{2+}$	4	3.101, 3.726	34, 180	146	[120, 121]
$[Pt_4(hyd)_4(NH_3)_8]$	4	3.131, 3.204	7, 180	161	[122]
$[Pt_4(C_4O_4)_4(NH_3)_8]$	4	3.162, 3.197	38, 180	160	[123]
$[Pd_2Pt_2(meu)_4(en)_2(NH_3)_4]^{4+}$	4	2.927, 3.225	17, 180	159	[124]

these compounds combine to give deviations from linearity that are in many cases small (i.e., $\theta > 170^\circ$) and thus unsuitable for a qualitative theoretical study. Therefore, we focus on compounds of the type $[RhX_2L_2]$ and [Rh(chelate)L_2], where "chelate" stands for bipyridine, acetylacetonato, or oxalato ligands, and X and L are monodentate ligands. In Figure 7 we present the distribution of the chain angles separately for those compounds with ligands of similar π-acceptor/π-donor properties (white bars) and for those in which two donor atoms have markedly better π-acidic character than the other two atoms (shaded bars), such as $[M(acac)(CO)_2]$, $[M(ox)(CO)_2]$, or $[M(bipy)Cl_2]$. Compounds with bridging ligands or with $M \cdots M$ distances longer than 3.5 Å are not included. Figure 7 clearly shows that only compounds with ligand sets showing different π-acidic characteristics are kinked.

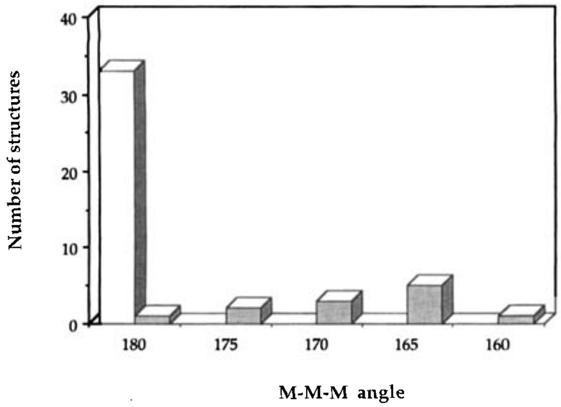

Figure 7. Distribution of the chain angle (θ, see Scheme 1) for compounds of the types $[RhX_2L_2]$ and [Rh(chelate)L_2] (X and L monodentate ligands). The white bars correspond to compounds with ligands of similar π-acceptor/π-donor properties. The shaded bars correspond to complexes in which two ligands have markedly better π-acidic character than the other two, such as $[M(acac)(CO)_2]$, $[M(ox)(CO)_2]$, or $[M(bipy)Cl_2]$. Compounds with bridging ligands or with $M \cdots M$ distances longer than 3.5 Å have been omitted.

We studied the loss of linearity in the M-M-M backbone of $[Rh(acac)(CO)_2]$ in its most stable conformation ($\tau = 180^\circ$), by performing EH tight-binding band calculations using a $Rh \cdots Rh$ distance of 3.3 Å. Note that for this compound one can envisage two different bending distortions, in which the acac ligands of neighboring molecules approach each other or separate. In our calculations it is the former that is the stabilizing chain distortion (Scheme 10). The displacement of successive monomers in parallel planes would make the $M \cdots M$ distance increase with decreasing θ, whereas a bending distortion keeping the $M \cdots M$ distance constant would result in changes in the interligand distances. Since the energies obtained from EH calculations are particularly unreliable when bonding distances are changed, we studied the two alternative distortions with similar qualitative results: the optimized value for θ is 153° when the distance between molecular planes is frozen at 3.40 Å, and 166° when the $M \cdots M$ distance is kept constant at the same value. This result is in excellent agreement with the geometry found experimentally for the analogous Rh compounds obtained by Schurig and co-workers (see Table 3). It is noteworthy that the observed distortion would be expected to be less favorable based only on the steric repulsions between the substituents in the acac ligands.

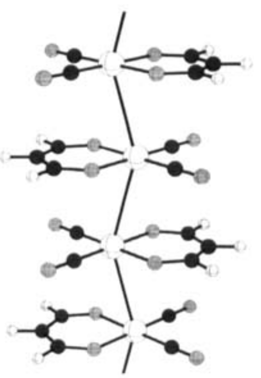

Scheme 10. Most stable chain geometry calculated for $[Rh(acac)(CO)_2]$.

We now want to address the question of whether the stabilization of the nonlinear geometry of $[Rh(acac)(CO)_2]$ is explained by interligand interactions or by the bonding $M \cdots M$ interaction discussed above. It should be stressed that, in addition to an energy decrease with bending, an increase in the calculated $M \cdots M$ overlap population is observed, reaching a maximum at $\theta \approx 167^\circ$. Of the three contributions to the $M \cdots M$ σ interaction (see Scheme 4), the four-electron repulsion ① is made weaker, because of the decreased overlap between the d_{z^2} orbitals. Similarly, interaction ② becomes less attractive. However, the metal–metal/donor–acceptor interaction mediated by the π^* orbitals of the π-acidic ligands, ③, is reinforced upon bending. Because of the different π-acidic properties of $acac^-$ and the carbonyls, the π^*_{CO} orbitals mix with d_{xz}, hybridized as shown in Scheme 5. Hence, the interaction ③ becomes more bonding upon chain bending, owing to the improved overlap between the d_{z^2} and π^*_{CO} orbitals (Scheme 11).

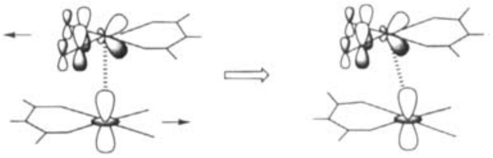

Scheme 11. Improved overlap with bending between d_{z^2} and π^*_{CO} orbitals of $[Rh(acac)(CO)_2]$.

Appendix

Computational Details: Extended Hückel calculations of molecular orbitals for monomers and dimers[125,126] and tight-binding electronic band structure calculations for chains[9,127] were carried out using the modified Wolfsberg–Helmholz formula for the nondiagonal matrix elements.[128] The CACAO[129] program was used for MO calculations, whereas EHMACC[130] and YAeHMOP[131] codes were employed for the band calculations. Atomic parameters were taken from the literature for Rh,[103] Pt,[132] (C, N, O, H),[126] S,[133] and Cl.[134] Total energy and density of states for chains were calculated by using a mesh of 100 k-points in the irreducible part of the Brillouin zone. Band calculations were carried out for the chain compounds presented in Table 5. The results of band calculations were in agreement with the orbital picture discussed for the dimers, as seen through the analysis of the different contributions to the DOS and COOP curves (not shown). In molecular orbital and band structure calculations all complexes were taken as planar with L-M-L angles of 90° for all nonchelating ligands. The following bond lengths were used: Pt–S = 2.32, Pt–O = 2.00, Pt–CO = 1.85, Pt–CN = 1.94, Pt–Cl = 2.40, Rh–C = 1.80, Rh–O = 2.05, Rh–Cl = 2.40, C–O = 1.15, C–N = 1.15, C–S = 1.68, C–H = 1.09 Å. Other bond lengths and angles used are summarized in Scheme 12.

Structural Database Search: Structural data was collected through a systematic search of the Cambridge Structural Database[135] for square-planar compounds of general formula ML_4, in which M was defined as a metal at its oxidation state with a d^8 configuration: Co^I, Rh^I, Ir^I, Ni^{II}, Pd^{II}, Pt^{II}, Au^{III}, Ru^0, and Os^0. The torsion angle τ was taken as the average of the four smaller nonequivalent torsion angles.

© VCH Verlagsgesellschaft mbH, D-69451 Weinheim, 1997
0947-6539/97/0304-0662 $ 17.50+.50/0

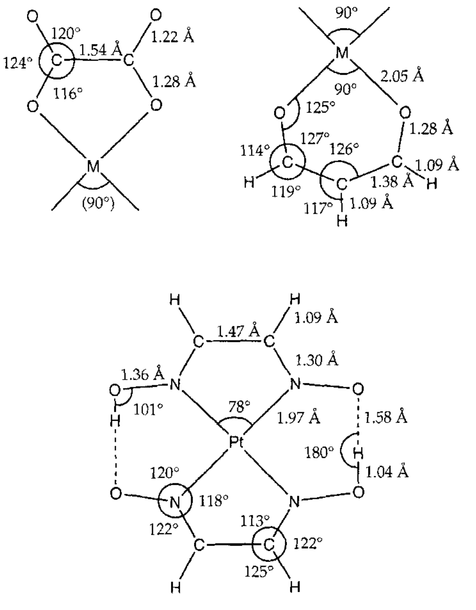

Scheme 12. Bond lengths and angles used in molecular orbital and band structure calculations.

Abbreviations: acac: acetylacetonato (1 −); acamph: (1*S*,1*R*)-3-trifluoroacetylcamphorato(1 −); bipy: 2,2′-bipyridine; bomp: 2-(2′-benzoxazolyl)-5-methyl-phenyl; bph: 2,2′-biphenyl; btmp: 2-(2′-benzothiazolyl-5-methyl-phenyl; Hbzgly: benzodioximato(1 −); cod: 1,5-cyclooctadiene; Hdmg: dimethylglyoximato(1 −); dpmp: bis((diphenylphosphino)methyl)phenylphosphine; Dtc: dithiocarbamate(1 −); en: 1,2-ethylenediamine; gcamph: 3,3′-hexafluoroglutarylbis((1*R*)-camphorato)(2 −); gly: glyoximato; hnapy: 2-oxo-1,8-naphtopyridinato(1 −); hp: 2-oxopyridinato(1 −); hyd: 1-methylhydantoinato(1 −); im: imidazole; mdcbi: 2-methylimidazole-4,5-dicarboxylato(3 −); menth: (1*RS*,4*SR*)-trifluoroacetylmenthonato(1 −); mcu: 1-methyluracilato(1 −); mpyt: 4-methyl-2-pyridinethiolato(1 −); ox: oxalato(2 −); pyrr: 2-pyrrolidonato(1 −); pyt: 2-pyridinethiolato(1 −); pz: pyrazolato(1 −); tfbb: tetrafluorobenzobarrelene; ttz: teterazolato(1 −); tz: triazolato(1 −).

Acknowledgments: Financial support for this work was provided by DGICYT through grant PB95-0848 and by the Comissionat per Universitats i Recerca (Generalitat de Catalunya) through grant GRQ94-1077. G. A. thanks CIRIT for a doctoral grant. The authors thank L. A. Oro for providing them with unpublished data.

Note added in proof: The structure of the long-known [PtCl$_2$(CO)$_2$] complex has only recently been determined (F. Bagnoli, D. B. Dell'Amico, F. Calderazzo, U. Englert, F. Marchetti, G. E. Herberich, N. Pasqualetti, S. Ramello, *J. Chem. Soc. Dalton Trans.* **1996**, 4317) and its structural parameters (Pt ⋯ Pt = 3.378 Å, τ = 180° and θ = 162.9) provide a nice illustration of the features discussed in this paper.

Received: October 8, 1996 [F 486]

---

[1] L. K. Monteith, L. F. Ballard, C. G. Pitt, B. K. Klein, L. M. Slifkin, J. P. Collman, *Solid State Commun.* **1968**, *6*, 301.
[2] K. Krogmann, *Angew. Chem. Int. Ed. Engl.* **1969**, *8*, 35.
[3] T. W. Thomas, A. E. Underhill, *Chem. Soc. Rev.* **1972**, *1*, 99.
[4] J. S. Miller, A. J. Epstein, *Prog. Inorg. Chem.* **1976**, *20*, 1.
[5] H. J. Keller, *Chemistry and Physics of One-Dimensional Metals*, Plenum Press, New York, **1977**.
[6] J. M. Williams, *Adv. Inorg. Chem. Radiochem.* **1983**, *26*, 235.
[7] T. W. Thomas, A. E. Underhill, *J. Chem. Soc. Chem. Commun.* **1969**, 725.
[8] P. S. Gomm, T. W. Thomas, A. E. Underhill, *J. Chem. Soc. A* **1971**, 2154.
[9] M.-H. Whangbo, R. Hoffmann, *J. Am. Chem. Soc.* **1978**, *100*, 6093.
[10] S. Alvarez, R. Vicente, R. Hoffmann, *J. Am. Chem. Soc.* **1985**, *107*, 6253.
[11] S. Alvarez, E. Canadell, *Solid State Commun.* **1986**, *50*, 141.
[12] G. Aullón, P. Alemany, S. Alvarez, *Inorg. Chem.* **1996**, *35*, 5061.
[13] J. J. Novoa, G. Aullón, P. Alemany, S. Alvarez, *J. Am. Chem. Soc.* **1995**, *117*, 7169.
[14] J. Y. Saillard, R. Hoffmann, *J. Am. Chem. Soc.* **1984**, *106*, 2006.
[15] H. Isci, W. R. Mason, *Inorg. Chem.* **1974**, *13*, 1175.
[16] H. Isci, W. R. Mason, *Inorg. Chem.* **1975**, *14*, 905, 913.
[17] H. Isci, Ö. Dag, W. R. Mason, *Inorg. Chem.* **1993**, *32*, 3909.
[18] H. Takazawa, S. Ohba, Y. Saito, M. Sano, *Acta Crystallogr. Sect. B* **1990**, *46*, 166.
[19] G. Gliemann, H. Yersin, *Struct. Bonding (Berlin)* **1985**, *62*, 87.
[20] K. Krogmann, *Z. Naturforsch. Teil B* **1968**, *23*, 1012.
[21] P. L. Johnson, T. R. Koch, J. M. Williams, *Acta Crystallograllogr. Sect. B* **1977**, *33*, 1976.
[22] J. Ledent, *Bull. Soc. Roy. Sci. Liège* **1972**, *431*, 537.
[23] P. Day, A. F. Orchard, A. J. Thomson, R. J. P. Williams, *J. Chem. Phys.* *1965*, *42*, 1973.
[24] D. S. Martin, Jr., *Inorg. Chim. Acta Rev.* **1971**, *5*, 107.
[25] N. Masciocchi, M. Moret, P. Cairati, F. Ragaini, A. Sironi, *J. Chem. Soc. Dalton Trans.* **1993**, 471.
[26] F. Bonati, L. A. Oro, M. T. Pinillos, C. Tejel, M. C. Apreda, C. Foces-Foces, F. H. Cano, *J. Organomet. Chem.* **1989**, *369*, 253.
[27] M. J. Decker, D. O. K. Kjeldsted, S. R. Stobart, M. J. Zaworotho, *J. Chem. Soc. Chem. Commun.* **1983**, 1525.
[28] A. H. Reis, Jr., V. S. Hagley, S. W. Peterson, *J. Am. Chem. Soc.* **1977**, *99*, 4184.
[29] A. H. Reis, Jr., in *Extended Linear Chain Compounds* ; *Vol. 1*, (Ed.: J. S. Miller), Plenum Press, New York, **1982**, p. 157.
[30] F. K. Larsen, R. G. Hazell, S. E. Rasmussen, *Acta Chem. Scand.* **1969**, *23*, 61.
[31] E. Holt, K. J. Watson, *Acta Chem. Scand.* **1969**, *23*, 14.
[32] L. Dupond, *Acta Crystallogr. Sect. B* **1970**, *26*, 964.
[33] J. Ledent, *Bull. Soc. Roy. Sci. Liège* **1974**, *43*, 172.
[34] K. Krogmann, D. Stephan, *Z. Anorg. Allgem. Chem.* **1968**, *362*, 290.
[35] P. L. Johnson, R. L. Musselman, J. M. Williams, *Acta Crystallogr. Sect. B* **1977**, *33*, 3155.
[36] R. L. Maffly, P. L. Johnson, J. M. Williams, *Acta Crystallogr. Sect. B.* **1977**, *33*, 884.
[37] L. Dupont, *Bull. Soc. Roy. Sci. Liège* **1969**, *38*, 509.
[38] T. R. Koch, P. L. Johnson, J. M. Williams, *Inorg. Chem.* **1977**, *16*, 640.
[39] D. M. Washecheck, S. W. Peterson, A. H. Reis, Jr., J. M. Williams, *Inorg. Chem.* **1976**, *15*, 74.
[40] H. H. Otto, H. Schulz, K. H. Thiemann, H. Yersin, G. Gliemann, *Z. Naturforsch. Teil B* **1977**, *32*, 127.
[41] P. L. Johnson, T. R. Koch, J. M. Williams, *Acta Crystallogr. Sect. B.* **1977**, *33*, 1293.
[42] L. Dupont, *Bull. Soc. Roy. Sci. Liège* **1967**, *36*, 40, 471.
[43] N. A. Bailey, E. Coates, G. B. Robertson, F. Bonati, R. Ugo, *J. Chem. Soc. Chem. Commun.* **1967**, 1041.
[44] P. W. DeHaven, V. L. Goedken, *Inorg. Chem.* **1979**, *18*, 827.
[45] G. C. Gorden, P. W. DeHaven, M. C. Weiss, V. L. Goedken, *J. Am. Chem. Soc.* **1978**, *100*, 1003.
[46] C. G. Pitt, L. K. Monteith, L. F. Ballard, J. P. Collman, J. C. Morrow, W. R. Roper, D. Ulkü, *J. Am. Chem. Soc.* **1966**, *88*, 4286.
[47] V. Schurig, *Angew. Chem. Int. Ed. Engl.* **1981**, *20*, 807.
[48] V. Schurig, W. Pille, W. Winter, *Angew. Chem. Int. Ed. Engl.* **1983**, *22*, 327.
[49] V. Schurig, W. Pille, K. Peters, H. G. von Schnering, *Mol. Cryst. Liq. Cryst.* **1985**, *120*, 385.
[50] V. Schurig, H. Gaus, P. Scheer, L. Walz, H. G. von Schnering, *Angew. Chem. Int. Ed. Engl.* **1989**, *28*, 1019.
[51] J. Real, J. C. Bayón, F. J. Lahoz, J. A. López, *J. Chem. Soc. Chem. Commun.* **1989**, 1889.
[52] A. E. Underhill, D. M. Watkins, J. M. Williams, K. Carneiro, in *Extended Linear Chain Compounds, Vol. 1* (Ed.: J. S. Miller), Plenum Press, New York, **1982**, p. 119.
[53] Ö. Bekaroglu, M. El Sharif, H. Endres, H. J. Keller, *Acta Crystallogr. Sect. B* **1976**, *32*, 2983.
[54] A. Kobayashi, Y. Sasaki, H. Kobayashi, *Bull. Chem. Soc. Jpn.* **1979**, *52*, 3682.
[55] A. Kobayashi, H. Kondo, Y. Sasaki, H. Kobayashi, A. E. Underhill, D. M. Watkins, *Bull. Chem. Soc. Jpn.* **1982**, *55*, 2074.
[56] K. Krogmann, *Z. Anorg. Allg. Chem.* **1968**, *358*, 97.
[57] A. J. Schultz, A. E. Underhill, J. M. Williams, *Inorg. Chem.* **1978**, *17*, 1313.
[58] M. S. Hussain, B. E. V. Salinas, E. O. Schlemper, *Acta Crystallogr. Sect. B* **1979**, *35*, 628.
[59] C. Bellitto, M. Bonamico, G. Dessy, V. Fares, A. Flamini, *J. Chem. Soc. Dalton Trans.* **1987**, 35.
[60] L. D. Brown, D. W. Kalina, M. S. McClure, S. Schultz, S. L. Ruby, J. A. Ibers, *J. Am. Chem. Soc.* **1979**, *101*, 2937.
[61] L. E. Godycki, R. E. Rundle, *Acta Crystallogr.* **1953**, *6*, 487.
[62] I. Leichert, J. Weiss, *Acta Crystallogr. Sect. B* **1975**, *31*, 2877.
[63] H. Endres, A. Bongart, *Acta Crystallogr. Sect. B* **1985**, *41*, 1605.
[64] H. Endres, *Acta Crystallogr. Sect. B* **1979**, *35*, 625.
[65] H. Endres, H. J. Keller, R. Lehmann, J. Weiss, *Acta Crystallogr. Sect. B* **1976**, *32*, 627.
[66] M. S. Hussain, S. A. A. Al-Hamoud, M. Z. El-Faer, A. Khan, *J. Coord. Chem.* **1985**, *14*, 91.
[67] H. Endres, *Acta Crystallogr. Sect. B* **1980**, *36*, 1347.

[68] M. Calleri, G. Ferraris, D. Viterbo, *Inorg. Chim. Acta* **1967**, *1*, 297.
[69] H. Endres, *Acta Crystallogr. Sect. B* **1982**, *38*, 1601.
[70] M. Megnamisi-Belombe, *J. Solid State Chem.* **1979**, *27*, 389.
[71] J. L. Briansó, M. de Matheus, *Afinidad* **1982**, *39*, 271.
[72] E. Frasson, C. Panattoni, R. Zannetti, *Acta Crystallogr.* **1959**, *12*, 1027.
[73] H. Endres, M. Megnamisi-Belombe, H. J. Keller, J. Weiss, *Acta Crystallogr. Sect. B* **1976**, *32*, 457.
[74] G. Ferraris, D. Viterbo, *Acta Crystallogr. Sect B* **1969**, *25*, 2066.
[75] H. Endres, *Acta Crystallogr. Sect. B* **1982**, *38*, 1316.
[76] H. Endres, G. Liebich-Brody, *Z. Naturforsch. Teil B* **1986**, *41*, 137.
[77] K. Krogmann, *Z. Anorg. Allg. Chem.* **1966**, *346*, 188.
[78] H. Endres, G. Liebich-Brody, *Z. Naturforsch. Teil B* **1986**, *41*, 339.
[79] S. Huq, A. C. Skapski, *J. Cryst. Mol. Struct.* **1974**, *4*, 411.
[80] A. Elduque, C. Finistra, F. J. Lahoz, J. A. López, L. A. Oro, M. T. Pinillos, to be published.
[81] L. A. Oro, M. T. Pinillos, C. Tejel, M. C. Apreda, C. Foces-Foces, F. H. Cano, *J. Chem. Soc. Dalton Trans.* **1988**, 1927.
[82] L. A. Oro, M. T. Pinillos, C. Tejel, C. Foces-Foces, F. H. Cano, *J. Chem. Soc. Chem. Commun.* **1984**, 1687.
[83] L. A. Oro, M. T. Pinillos, C. Tejel, C. Foces-Foces, F. H. Cano, *J. Chem. Soc. Dalton Trans.* **1986**, 1087.
[84] B. M. Louie, S. J. Rettig, A. Storr, J. Trotter, *Can. J. Chem.* **1985**, *63*, 688.
[85] G. Net, J. C. Bayón, W. M. Butler, P. Rasmussen, *J. Chem. Soc. Chem. Commun.* **1989**, 1022.
[86] M. Maekawa, M. Munakata, S. Katagawa, M. Nakamura, *Anal. Sci.* **1991**, *7*, 521.
[87] Y.-H. Chen, J. W. Merkert, Z. Murtaza, C. Woods, D. P. Rillema, *Inorg. Chim. Acta* **1995**, *240*, 41.
[88] C.-M. Che, L.-Y. He, C.-Y. Poon, T. C. W. Mak, *Inorg. Chem.* **1989**, *28*, 3081.
[89] R. S. Osborn, D. Rogers, *J. Chem. Soc. Dalton Trans.* **1974**, 1002.
[90] W. B. Connick, L. M. Henling, R. E. Marsh, *Acta Crystallogr. Sect. B* **1996**, *52*, 817.
[91] G. Ciullo, O. Piovesana, *Inorg. Chem.* **1980**, *19*, 2871.
[92] M. Bonamico, G. Dessy, V. Fares, *J. Chem. Soc. Chem. Commun.* **1969**, 1106.
[93] M. Bonamico, G. Dessy, V. Fares, *J. Chem. Soc. Dalton Trans.* **1977**, 2315.
[94] O. Piovesana, C. Bellito, A. Flamini, P. F. Zanazzi, *Inorg. Chem.* **1979**, *18*, 2258.
[95] C. Bellitto, A. Flamini, O. Piovesana, P. F. Zanazzi, *Inorg. Chem.* **1980**, *19*, 3632.
[96] C. Bellitto, G. Dessy, V. Fares, A. Flamini, *J. Chem. Soc. Chem. Commun.* **1981**, 409.
[97] T. Kawamura, T. Ogawa, T. Yamabe, H. Masuda, T. Taga, *Inorg. Chem.* **1987**, *26*, 3547.
[98] Y. Ohashi, I. Hanazaki, S. Nagahura, *Inorg. Chem.* **1970**, *9*, 2551.
[99] H. Endres, N. Gottstein, H. J. Keller, R. Martin, W. Rodemer, W. Steiger, *Z. Naturforsch. Teil B* **1979**, *34*, 827.
[100] K. R. Mann, N. S. Lewis, R. M. Williams, H. B. Gray, J. G. Gordon, III, *Inorg. Chem.* **1978**, *17*, 828.
[101] K. R. Mann, J. A. Thich, R. A. Bell, C. L. Coyle, H. B. Gray, *Inorg. Chem.* **1980**, *19*, 2462.
[102] K. R. Mann, *Cryst. Struct. Commun.* **1981**, *10*, 451.
[103] R. Hoffmann, C. Minot, H. B. Gray, *J. Am. Chem. Soc.* **1984**, *106*, 2001.
[104] H. Takazawa, S. Ohba, Y. Saito, *Acta Crystallogr. Sect. B* **1988**, *44*, 580.
[105] J. R. Hester, *Acta Crystallogr. Sect. C* **1990**, *46*, 48.
[106] M. A. Ciriano, B. E. Villarroya, L. A. Oro, M. C. Apreda, C. Foces-Foces, F. H. Cano, *J. Organomet. Chem.* **1989**, *366*, 377.
[107] R. S. Dubis, J. P. Fackler, Jr., *Inorg. Chem.* **1985**, *24*, 3758.
[108] A. Tiripicchio, F. J. Lahoz, L. A. Oro, M. A. Ciriano, B. E. Villarroya, *Inorg. Chim. Acta* **1986**, *111*, L1.
[109] A. L. Balch, L. A. Fossett, J. K. Nagle, M. M. Olmstead, *J. Am. Chem. Soc.* **1988**, *110*, 6732.
[110] D. H. R. Barton, J. Khamsi, N. Ozoalik, J. Ribenspies, *Tetrahedron* **1990**, *46*, 3111.
[111] M. R. Churchill, H. J. Wasserman, G. J. Young, *Inorg. Chem.* **1980**, *19*, 762.
[112] K. Suzuki, K. Matsumoto, *Chem. Lett.* **1989**, 317.
[113] K. Matsumoto, H. Moriyama, K. Suzuki, *Inorg. Chem.* **1990**, *29*, 2096.
[114] L. S. Hollis, S. J. Lippard, *J. Am. Chem. Soc.* **1981**, *103*, 1230.
[115] L. S. Hollis, S. J. Lippard, *J. Am. Chem. Soc.* **1983**, *105*, 3494.
[116] G. Trotscher, W. Micklitz, H. Schöllhorn, U. Thewalt, B. Lippert, *Inorg. Chem.* **1990**, *29*, 2541.
[117] P. de Meester, A. C. Skapski, *J. Chem. Soc. Dalton Trans.* **1973**, 1194.
[118] L. S. Hollis, S. J. Lippard, *Inorg. Chem.* **1983**, *22*, 2600.
[119] K. Matsumoto, H. Miyamae, H. Moriyama, *Inorg. Chem.* **1989**, *28*, 2959.
[120] I. Kinoshita, Y. Yasuba, K. Matsumoto, S. Ooi, *Inorg. Chim. Acta* **1983**, *80*, L13.
[121] K. Umakoshi, I. Kinoshita, Y. Fukui-Yasuba, K. Matsumoto, S. Ooi, H. Nakai, M. Shiro, *J. Chem. Soc. Dalton Trans.* **1989**, 815.
[122] J. P. Laurent, P. Leoage, F. Dahan, *J. Am. Chem. Soc.* **1982**, *104*, 7335.
[123] G. Bernadinelli, P. Castan, R. Soules, *Inorg. Chim. Acta* **1985**, *120*, 205.
[124] W. Micklitz, J. Riede, B. Muber, G. Müller, B. Lippert, *Inorg. Chem.* **1988**, *27*, 1979.
[125] R. Hoffmann, W. N. Lipscomb, *J. Chem. Phys.* **1962**, *36*, 2179, 2872.
[126] R. Hoffmann, *J. Chem. Phys.* **1963**, *39*, 1397.
[127] M.-H. Whangbo, R. Hoffmann, R. B. Woodward, *Proc. R. Soc. London Ser. A* **1979**, *366*, 23.
[128] J. H. Ammeter, H.-B. Bürgi, J. C. Thibeault, R. Hoffmann, *J. Am. Chem. Soc.* **1978**, *100*, 3686.
[129] C. Mealli, D. M. Proserpio, *J. Chem. Educ.* **1990**, *67*, 399.
[130] *EHMACC: Extended Hückel for Molecules and Crystals Calculations*, M.-H. Whangbo, M. Evain, T. Hughbanks, M. Kertesz, S. Wijeyesekera, C. Wilker, C. Zheng, R. Hoffmann, QCPE, Bloomington, IN, **1987**.
[131] *YAeHMOP—Yet Another Extended Hückel Molecular Orbital Package (1.1)*, G. Landrum, Cornell University, Ithaca, N. Y., **1995**.
[132] R. H. Summerville, R. Hoffmann, *J. Am. Chem. Soc.* **1976**, *98*, 7240.
[133] M. M. L. Chen, R. Hoffmann, *J. Am. Chem. Soc.* **1976**, *98*, 1647.
[134] R. Hoffmann, M. M. L. Chen, M. Elian, A. R. Rossi, D. M. P. Mingos, *Inorg. Chem.* **1974**, *13*, 2666.
[135] F. H. Allen, O. Kennard, R. Taylor, *Acc. Chem. Res.* **1983**, *16*, 146.